Mesoscopic approach to subcritical fatigue crack growth

Maycon S. Araújo[*] and André P. Vieira[†]
Departamento de Física Geral, Instituto de Física, Universidade de São Paulo, Caixa Postal 66318, 05314-970 São Paulo, SP, Brazil

José S. Andrade, Jr.[‡]
Departamento de Física, Universidade Federal do Ceará, Caixa Postal 6030, 60451-970 Fortaleza, CE, Brazil

Hans J. Herrmann[§]
Departamento de Física, Universidade Federal do Ceará, Caixa Postal 6030, 60451-970 Fortaleza, CE, Brazil
and Computational Physics, Institut für Baustoffe (IfB), ETH-Hönggerberg Schafmattstrasse 6, HIF E 12, CH-8093 Zürich, Switzerland
(Received 18 July 2016; published 27 October 2016)

We investigate a model for fatigue crack growth in which damage accumulation is assumed to follow a power law of the local stress amplitude, a form that can be generically justified on the grounds of the approximately self-similar aspect of microcrack distributions. Our aim is to determine the relation between model ingredients and the Paris exponent governing subcritical crack-growth dynamics at the macroscopic scale, starting from a single small notch propagating along a fixed line. By a series of analytical and numerical calculations, we show that, in the absence of disorder, there is a critical damage-accumulation exponent γ, namely $\gamma_c = 2$, separating two distinct regimes of behavior for the Paris exponent m. For $\gamma > \gamma_c$, the Paris exponent is shown to assume the value $m = \gamma$, a result that proves robust against the separate introduction of various modifying ingredients. Explicitly, we deal here with (i) the requirement of a minimum stress for damage to occur, (ii) the presence of disorder in local damage thresholds, and (iii) the possibility of crack healing. On the other hand, in the regime $\gamma < \gamma_c$, the Paris exponent is seen to be sensitive to the different ingredients added to the model, with rapid healing or a high minimum stress for damage leading to $m = 2$ for all $\gamma < \gamma_c$, in contrast with the linear dependence $m = 6 - 2\gamma$ observed for very long characteristic healing times in the absence of a minimum stress for damage. Upon the introduction of disorder on the local fatigue thresholds, which leads to the possible appearance of multiple cracks along the propagation line, the Paris exponent tends to $m \approx 4$ for $\gamma \lesssim 2$ while retaining the behavior $m = \gamma$ for $\gamma \gtrsim 4$.

DOI: 10.1103/PhysRevE.94.043003

I. INTRODUCTION

Fracture phenomena are quite common in nature and play a fundamental role in many situations of interest for science and technological applications [1,2]. Despite many advances in materials science and applied mechanics over the past decades, the full description of such problems remains a great challenge to physicists and engineers [3]. However, it is a well-known fact that the presence of cracks within a material can magnify by several times the effect of the external stresses applied, causing a strong reduction in its strength and inducing rupture at a stress very much lower than that needed to break the atomic bonds in a flawless, regular arrangement [3,4].

Scaling arguments developed by Griffith [5] show that a single crack, after reaching some critical length, will propagate spontaneously within the material, causing its catastrophic failure. Below that critical length, many kinds of external mechanisms occurring on relatively slow time scales can dominate the crack dynamics, defining a subcritical regime of crack growth [1]. Among those mechanisms, we highlight the occurrence of fatigue as the result of a progressive accumulation of damage throughout the material when submitted to cyclic load [1,3,6].

In general, subcritical fatigue crack propagation is well described by an empirical law largely used in engineering practice, known as the Paris (or Paris-Erdogan) law [7], which states that the growth rate of a linear crack under cyclic load follows a power law of the stress-intensity factor, with an exponent m,

$$\frac{da}{dN} = C(\Delta K)^m \sim a^{m/2}. \tag{1}$$

Here a is the crack half-length, N is the number of loading cycles applied to the material, da/dN is the crack-growth rate (proportional to the crack-tip speed), $\Delta K \equiv g\Delta\sigma_0\sqrt{\pi a}$ is the amplitude of the stress-intensity factor of the crack, $\Delta\sigma_0$ and g being the stress amplitude and a geometrical factor, respectively, while m (the Paris exponent) and C are parameters that may depend on both the material properties and the experimental conditions. Numerous experiments have confirmed the validity of this law over several orders of magnitude for a wide variety of materials and loading conditions [1,3].

Despite its simplicity and practical importance, a systematic understanding of this law on physical grounds is still lacking, especially as regards the determination of an explicit relation between the Paris exponent m and microscopic parameters of a given material. An intermediate step was taken by three of the authors of the present paper [8], who were able to show that the Paris law indeed emerges from a

[*]maycon@if.usp.br
[†]apvieira@if.usp.br
[‡]soares@fisica.ufc.br
[§]hans@ifb.baug.ethz.ch

damage-accumulation rule defined by a power law of the external stress amplitude, with a characteristic exponent γ, whose relation with the Paris exponent m can be determined via a combination of analytical and numerical calculations. Although such a damage-accumulation rule can be justified by invoking self-similarity concepts [9], a first-principles calculation of the damage-accumulation exponent γ for a given material remains challenging. Nevertheless, assuming such a damage-accumulation rule on phenomenological grounds, it is possible to show [8] that, in the absence of disorder, there is a critical damage-accumulation exponent γ, namely $\gamma_c = 2$, separating two distinct regimes of behavior for the Paris exponent m. For $\gamma > \gamma_c$, the Paris exponent assumes the value $m = \gamma$, while for $\gamma < \gamma_c$ a different linear relation, $m = 6 - 2\gamma$, is verified.

Our aim in this paper is to further explore the consequences of the dynamics associated with a power-law damage accumulation rule, both in the uniform limit and in combination with disorder in the local rupture thresholds. Regarding disorder, some progress has already been made in Ref. [10] by a mapping to a random-fuse problem, which was solved numerically. Here we combine results from linear-elastic fracture mechanics with an independent-crack approximation to perform a thorough study of the effects of disorder on the relation between the damage-accumulation exponent γ and the Paris exponent m. We also investigate the effects of introducing a healing mechanism that lowers the local damage throughout the material as time passes. We present evidence that the relation $m = \gamma$ for $\gamma > \gamma_c$ is robust against the separate introduction of various modifying ingredients, but that in the regime $\gamma < \gamma_c$ the Paris exponent is sensitive to the different ingredients added to the model, with rapid healing or a high minimum stress for damage leading to $m = 2$ for all $\gamma < \gamma_c$, while disorder leads to $m \approx 4$.

The paper is organized as follows. The basic ingredients of the model are presented in Sec. II, with the next two sections dedicated to investigating the uniform limit in the absence of healing. The behavior of the model in the presence of disordered local damage thresholds in discussed in Sec. V. Healing effects in the uniform limit are introduced and discussed in Sec. VI. The final section summarizes our findings.

II. THE BASIC MODEL

In the present section, we define the model and discuss schematically the dynamics of crack growth. The next sections deal with particular cases and extensions.

Following Ref. [8], we assume that a single thin elliptic crack is initially produced in an infinite two-dimensional sample of a linear-elastic material. The sample is subject to cyclic loading, with an external stress σ_0 transverse to the major axis of the crack. We further assume that the crack grows only along its major axis, so that crack propagation becomes essentially a one-dimensional problem, as shown in Fig. 1.

Along the crack line, we discretize space so that the crack grows by the rupture of elements of fixed length δr, and we assume that, when the crack has length $2a$, the element at position x experiences a stress given by $\sigma(x + \delta r; a)$. This assumption prevents the appearance of divergences in the stress field around the crack tip, and, to a first approximation, it is consistent with the fact that linear-elasticity theory must break down in the immediate vicinity of the crack tip, giving rise to a fracture process zone or plastic zone [1,11]. We assume in this work that the size of the fracture process zone is smaller than the discretization length δr. We also assume that the relaxation time of the material is much shorter than the period of the loading cycle, so that crack propagation can be investigated within a quasistatic approximation, according to which the system always reaches its equilibrium state between two successive crack-growth events.

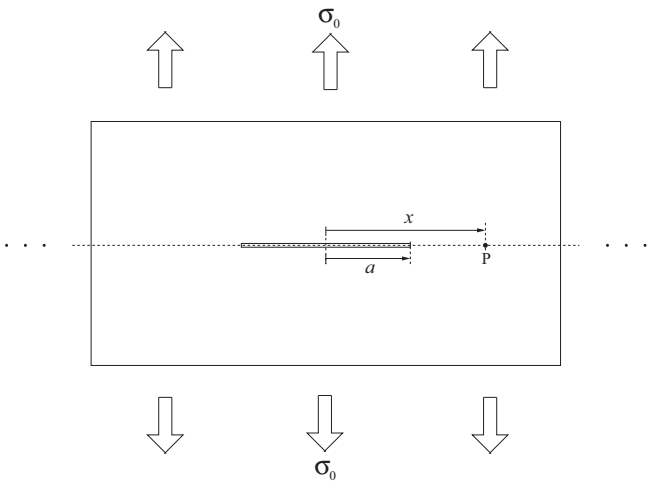

FIG. 1. A very thin elliptical crack of half-length a propagating along the direction of its major axis in a two-dimensional sample of material subject to an external stress σ_0. The crack propagation line is indicated by the dashed line, and x is the coordinate of a given point P relative to the midpoint of the crack.

In the continuum limit, and within linear-elasticity theory, the local stress $\sigma(x; a)$ along the crack line is given by [4]

$$\sigma(x; a) = \sigma_0 \frac{|x - x_0|}{\sqrt{(x - x_0)^2 - a^2}}, \tag{2}$$

where σ_0 is the external stress applied to the material, x is the coordinate of the point of interest, x_0 is the coordinate of the midpoint of the crack, and $2a$ is the crack length (see Fig. 2).

Sufficiently close to the crack tips, we obtain an asymptotic expression for $\sigma(x; a)$,

$$\sigma(x; a) \simeq \frac{K}{\sqrt{2\pi(|x - x_0| - a)}}, \tag{3}$$

defining the stress intensity factor $K = \sigma_0\sqrt{\pi a}$ for this particular geometry.

We postulate that cyclic loading with an external stress amplitude $\Delta\sigma_0 \equiv \sigma_{0,\max} - \sigma_{0,\min}$ leads to fatigue damage accumulation in each element along the crack line according to the rule

$$\delta F(x; a) = f_0 \delta t(a) [\Delta\sigma(x; a)]^\gamma, \tag{4}$$

where $\delta F(x; a)$ is the damage increment in the element located at position x during the time interval $\delta t(a)$ when the crack remained with length $2a$, $\Delta\sigma(x; a)$ is the corresponding

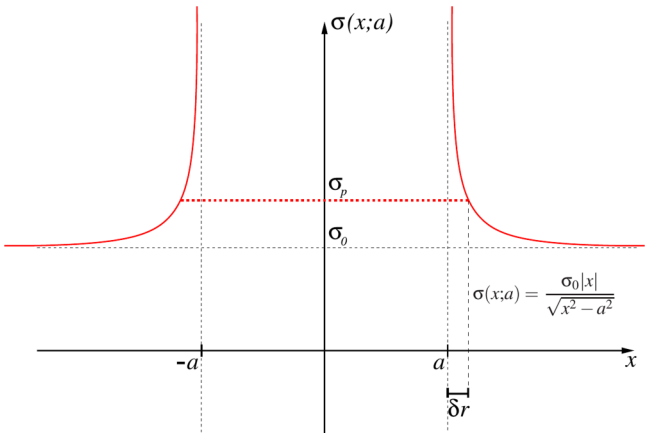

FIG. 2. Sketch of the stress field $\sigma(x;a)$ along the propagation line of the crack, whose midpoint is at $x_0 = 0$. Except for the presence of the crack, the medium is homogeneous. The cutoff value σ_p stands for the stress attributed to plastic effects within a zone around the crack tip, whose linear dimension is assumed here to be smaller than δr.

local stress amplitude, γ is a phenomenological damage accumulation exponent, and f_0 is a constant setting the time scale, being proportional to the inverse duration of the loading cycle; see Fig. 3 for an illustration.

Therefore, the damage at position x when the crack is about to grow from length $2a$ is given by the relation

$$F(x;a) = F(x;a') + \delta F(x;a), \tag{5}$$

in which $2a'$ is the previous crack length. When the crack always advances symmetrically with respect to the midpoint of the initial crack, we have $a' = a - \delta r$.

A heuristic motivation for the power-law dependence of the damage increment can be formulated by invoking concepts of self-similarity and fractality commonly observed in spatial patterns related to crack propagation and fragmentation processes [9,12–16], and assuming that the most important contribution to damage accumulation comes from the local stress amplitude.

Finally, we assume that an element at position x ruptures when the corresponding accumulated damage reaches a threshold $F_{\rm thr}(x)$. In the uniform limit, $F_{\rm thr}(x) \equiv F_{\rm thr}$ for all x, elements break sequentially, starting from the initial crack tips, and the crack advances symmetrically. In the general case, as shown below, elements far from the crack tip can suffer early rupture, leading to irregular crack growth and to the presence of multiple cracks. In all cases, we focus on the growth of the initial crack—or *main* crack—which may involve secondary cracks when these coalesce with the main crack.

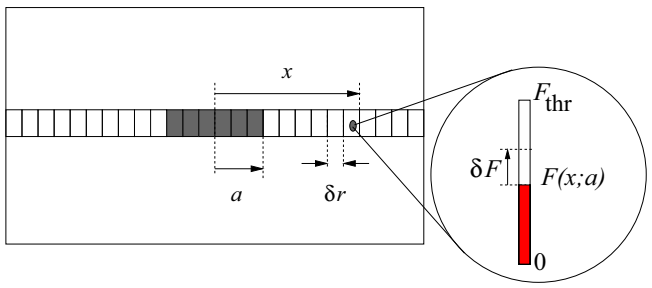

FIG. 3. Schematic diagram representing the damage-accumulation process for a given element at position x in a configuration with crack half-length a. The damage accumulated $F(x;a)$ is depicted by a life-bar with the level labeled in red that can receive a damage increment δF until it reaches the damage-accumulation threshold $F_{\rm thr}$.

The main crack advances when the accumulated damage in one or both elements at the crack tips reaches the corresponding threshold. Equations (4) and (5) allow the calculation of the number of cycles since the last growth event and of the updated accumulated damage along the crack line.

III. THE UNIFORM CASE

When all fatigue thresholds are equal, i.e., in the uniform limit, the monotonic behavior of the stress amplitude function $\Delta\sigma(x;a)$ (see Fig. 2) ensures the existence of a single crack along the whole rupture process. Furthermore, the crack always advances symmetrically, with elements at both crack tips breaking simultaneously. As already shown in Ref. [8], the iteration of Eqs. (4) and (5), along with the crack-growth condition, lead to a crack growth dynamics reproducing the Paris law, as illustrated in Fig. 4.

In the thermodynamic limit (i.e., for system sizes $L \to \infty$), the relation between the Paris exponent m and the damage-accumulation exponent γ is a piecewise-linear function

$$m(\gamma) = \begin{cases} 6 - 2\gamma, & \gamma \leqslant \gamma_c; \\ \gamma, & \gamma > \gamma_c, \end{cases} \tag{6}$$

with

$$\gamma_c = 2.$$

This follows from both analytical calculations for $\gamma > \gamma_c$ (see below) and from a finite-size scaling analysis of numerical calculations, according to

$$m(\gamma;L) - \gamma_c = \begin{cases} L^{-y}\,\mathcal{F}_-(|\gamma - \gamma_c|L^y), & \gamma < \gamma_c, \\ L^{-y}\,\mathcal{F}_+(|\gamma - \gamma_c|L^y), & \gamma > \gamma_c. \end{cases} \tag{7}$$

Here the system size L is the number of discretized elements up to which the calculations are iterated, $\mathcal{F}_\pm$ are scaling functions, and y is an exponent to be determined from the best data collapse of properly rescaled plots according to Eq. (7). As shown in Fig. 5, this finite-size-scaling hypothesis is nicely reproduced by numerical data for all values of γ.

The critical value $\gamma_c = 2$ of the damage-accumulation exponent is related to the divergence of the stress integral along the crack line, as shown by the analytical calculations presented below. It separates two regimes, one dominated by damage accumulation mostly around the crack tip, which happens for $\gamma \gg 1$, and one in which damage accumulation occurs more uniformly along the crack line, as in the limiting case $\gamma \to 0$.

An alternative method to obtain the thermodynamic limit from the numerical results comes from an analysis of crack-tip velocity versus crack length for a single value of γ, according

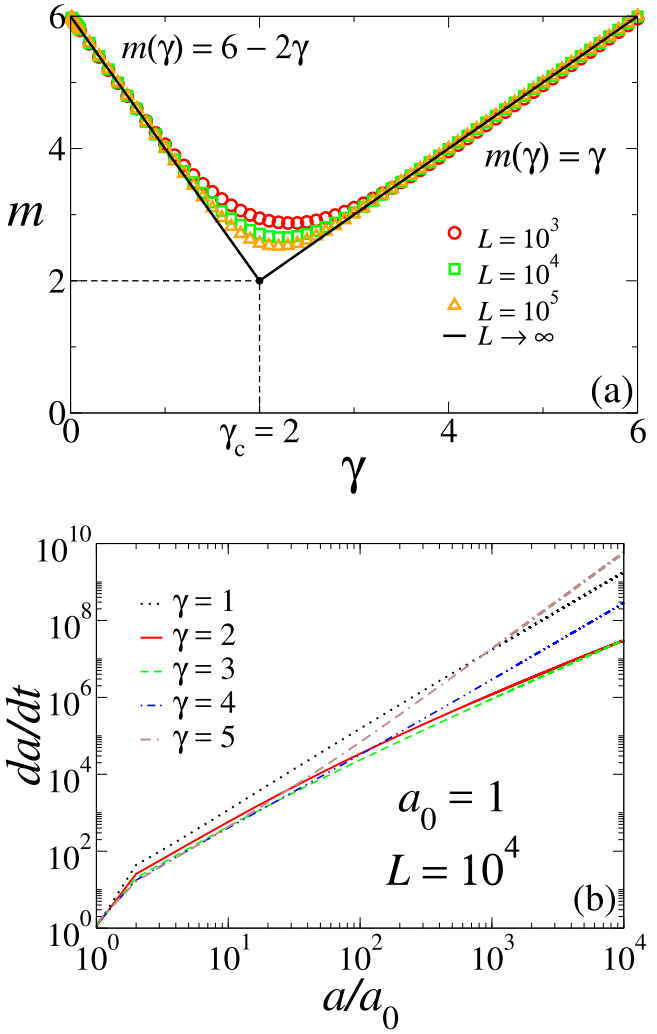

FIG. 4. Top: numerical dependence of the Paris exponent m on the damage-accumulation exponent γ for system sizes ranging from $L = 10^3$ to 10^5. The solid line corresponds to an extrapolation of the results to the thermodynamic limit assuming the finite-size scaling hypothesis given by Eq. (7). Bottom: typical curves of da/dt as a function of a/a_0 for several values of the damage-accumulation exponent γ.

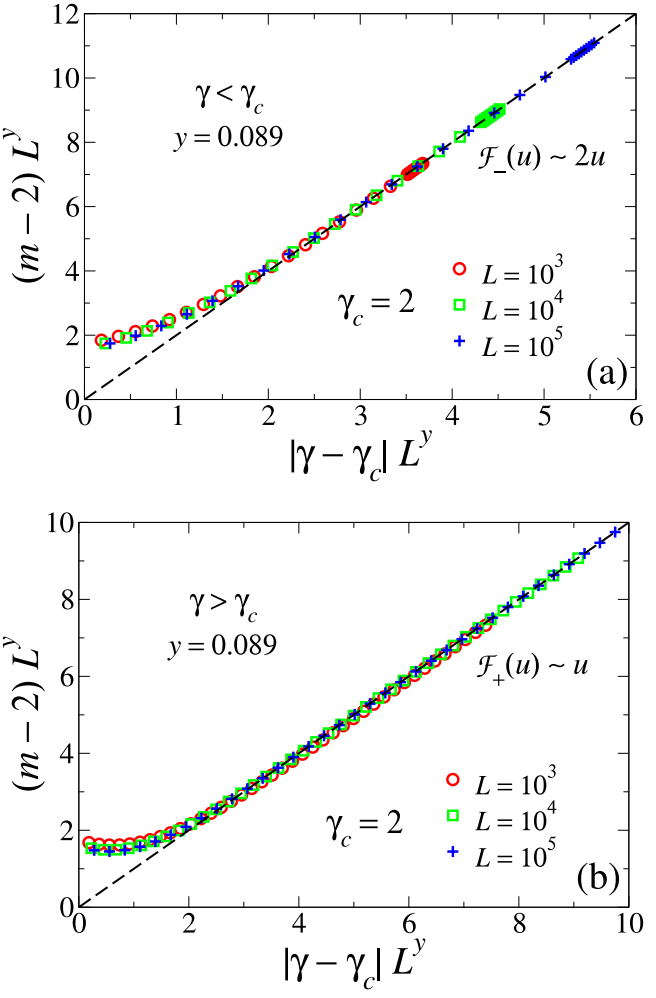

FIG. 5. Scaling plots of the dependence of m on γ and L, following Eq. (7), for different system sizes ranging from $L = 10^3$ to 10^5. Top: $\gamma < \gamma_c = 2$. Bottom: $\gamma > \gamma_c = 2$.

to the finite-size scaling hypothesis

$$L^{-m/2}\,\frac{da}{dt} \sim \left(\frac{a}{L}\right)^{m/2}, \tag{8}$$

where now m is chosen so as to produce the best data collapse of the rescaled curves, as illustrated in Fig. 6. This yields a continuous curve (not shown in Fig. 4), which agrees quite well with the previous piecewise linear prediction, except in the neighborhood of γ_c, where logarithmic corrections to a simple power-law behavior are expected to be relevant. Nevertheless, this alternative method turns out to be less susceptible to statistical fluctuations, and it will be used to evaluate the Paris exponent in the presence of disorder (see Sec. V).

Analytical calculations

A few analytical results for the uniform limit can be derived from a recursion relation obtained by eliminating $\delta t(a)$ using Eqs. (4) and (5) in order to compute the accumulated damage at the crack tip for each crack length.

In the uniform limit, as both crack tips always advance a single element at a time, after n iterations the crack length is $2a_n$, with

$$a_n = a_0 + n\delta r.$$

Here a_0 represents the initial size of the crack, which we assume to be larger than the minimum crack size associated with $\Delta K_{\rm thr}$, the threshold value of the stress-intensity factor at which a fatigue crack propagates at a detectable rate. For smaller sizes, crack growth proceeds at a very slow rate (see, e.g., Ref. [6], Chap. 2), below one atomic length per loading cycle, and our mesoscopic approach is inapplicable. Therefore, we expect that our results only apply to the Paris regime of fatigue crack propagation.

If we define

$$F_n \equiv F(a_{n+1}, a_{n-1}),$$

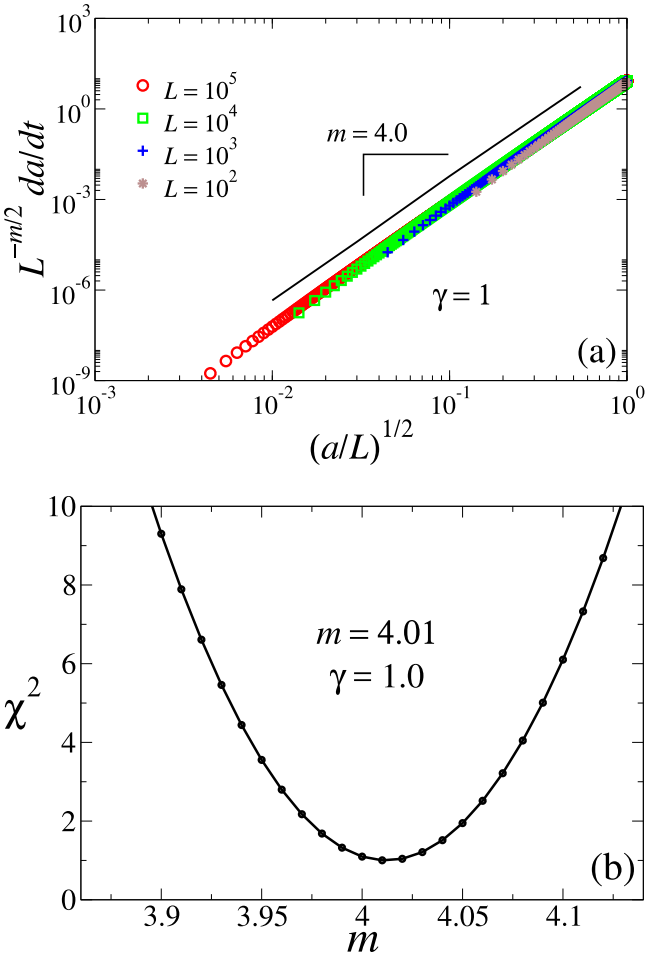

FIG. 6. Top: scaling plots of the dependence of da/dt on a and L for different system sizes ranging from $L = 10^2$ to 10^5, with $\gamma = 1$. Bottom: mean-square error of the data collapse as a function of the rescaling parameter m, showing a minimum very close to $m = 4$. The mean-square error is calculated by summing squares of relative deviations of rescaled ordinates for all rescaled values of abscissas, between all possible pairs of data sets.

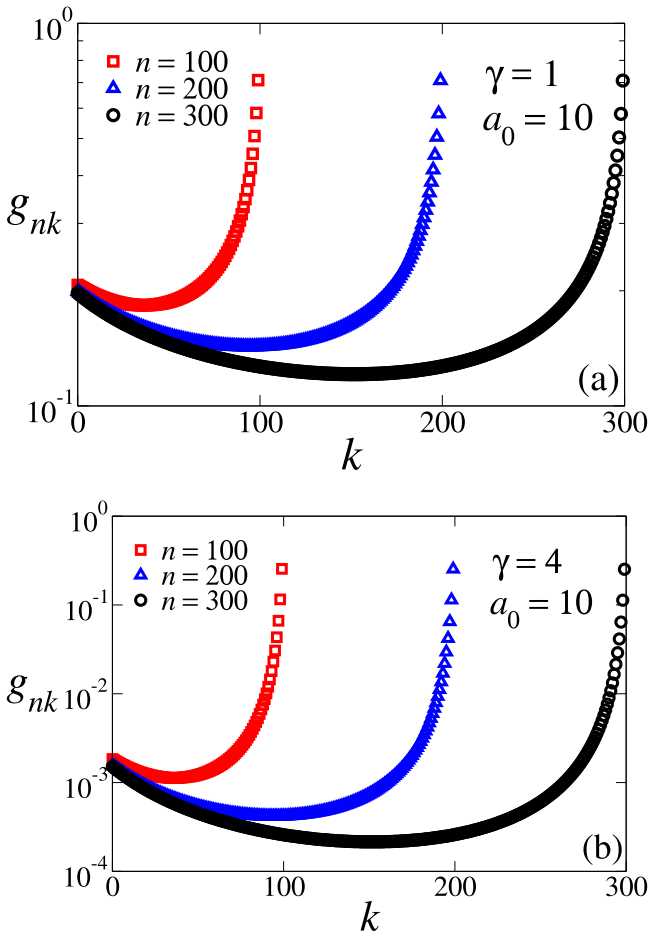

FIG. 7. Typical behavior of the stress amplitude amplitude ratio g_{nk} for a few values of the damage-accumulation exponent γ. Top: $\gamma = 1$. Bottom: $\gamma = 4$.

combining Eqs. (4) and (5) with the crack-growth condition leads to the time elapsed between consecutive rupture events,

$$\delta t(a_n) = \frac{F_{\rm thr}(1 - G_n)}{f_0[\Delta\sigma(a_{n+1}; a_n)]^\gamma}, \tag{9}$$

and to the rescaled recursion relation

$$G_n \equiv \frac{F_n}{F_{\rm thr}} = \sum_{k=1}^{n} g_{nk}(1 - G_{k-1}), \quad n > 0, \tag{10}$$

with $G_0 = 0$ and

$$g_{nk} \equiv \left[\frac{\Delta\sigma(a_0 + (n+1)\delta r; a_0 + (k-1)\delta r)}{\Delta\sigma(a_0 + k\delta r; a_0 + (k-1)\delta r)}\right]^\gamma. \tag{11}$$

Notice that g_{nk} is related to the ratio between the stress amplitudes at two different times in the rupture process, and that the asymptotic behavior of the rescaled accumulated damage G_n at the crack tip must be taken into account in order to estimate the crack-growth rate

$$\frac{da}{dN} \sim \frac{\delta r}{\delta t(a)} \sim \frac{1}{\delta t(a)}.$$

The asymptotic behavior of G_n is related to the asymptotic behavior of g_{nk}, which is given by

$$g_{nk} \sim \begin{cases} (2\delta r/a_0)^{\gamma/2}, & k\delta r \ll a_0 \ll n\delta r; \\ (2/k)^{\gamma/2}, & a_0 \ll k\delta r \ll n\delta r; \\ (n-k+2)^{-\gamma/2}, & a_0 \ll k\delta r \approx n\delta r. \end{cases} \tag{12}$$

Notice that g_{nk} assumes its largest values for k approaching n, as shown in Fig. 7.

If G_n approaches a value G^* smaller than unity as $n \to \infty$, it follows from Eqs. (10) and (12) that we can write

$$G^* \approx (1 - G^*) \sum_{k=1}^{\infty} (n-k+2)^{-\gamma/2} \equiv (1 - G^*) s_\infty(\gamma), \tag{13}$$

with

$$s_\infty(\gamma) = \begin{cases} \zeta\left(\frac{\gamma}{2}\right) - 1, & \gamma > 2; \\ \infty, & \gamma \leqslant 2, \end{cases} \tag{14}$$

where $\zeta(x)$ is the Riemann zeta function.

Therefore, for $\gamma > 2$ we have

$$G^* \approx \frac{s_\infty(\gamma)}{1+s_\infty(\gamma)} \quad \Rightarrow \quad \frac{da_n}{dt} \approx \frac{a_n^{\gamma/2}}{1-G^*} \sim a_n^{\gamma/2}, \tag{15}$$

yielding $m = \gamma$. However, this analysis breaks down for $\gamma < 2$, since G^* approaches unity as $\gamma \to 2^+$.

Nevertheless, for $\gamma \to 0^+$ we can write

$$\begin{aligned}[\Delta\sigma(x;a_n)]^\gamma &= \exp\{\ln[\Delta\sigma(x;a_n)]^\gamma\} \\ &\approx 1 + \ln[\Delta\sigma(x;a_n)]^\gamma,\end{aligned}$$

from which, by using Eqs. (10) and (12), we obtain, for $n > 1$,

$$G_n \approx 1 + \ln\left(\frac{g_{n,1}}{g_{n-1,1}}\right) \tag{16}$$

and

$$\frac{g_{n,1}}{g_{n-1,1}} \approx 1 - \gamma\left(\frac{a_0}{\delta r}\right)^2 n^{-3}. \tag{17}$$

Therefore, as $\gamma \to 0^+$ we have

$$\delta t(a_n) \sim \frac{1-G_n}{a_n^{\gamma/2}} \sim -\ln\left(\frac{g_{n,1}}{g_{n-1,1}}\right) \sim \gamma a_n^{-3} \tag{18}$$

so that we obtain a Paris exponent $m = 6$, in agreement with the numerical results. Notice, however, that the multiplicative coefficient in the Paris law expression, which in this limit is proportional to γ^{-1}, diverges as $\gamma \to 0$, in agreement with the expectation of sudden rupture when the damage threshold is reached simultaneously at all points.

IV. THE UNIFORM CASE WITH A MODIFIED DAMAGE-ACCUMULATION RULE

In analogy with modifications of the Paris law suggested by crack-closure phenomena, related to factors such as plasticity, roughness, and oxidation, which imply an effective reduction of the stress-intensity amplitude [6,17], the damage-accumulation rule can be modified to accommodate a threshold stress amplitude needed to induce local damage. This can be done by rewriting Eq. (4) in the form

$$\delta F(x;a) = f_0 \delta t(a)[\Delta\sigma_{\text{eff}}(x;a)]^\gamma, \tag{19}$$

with an effective stress amplitude

$$\Delta\sigma_{\text{eff}}(x;a) = \Delta\sigma(x;a) - b\Delta\sigma_0, \tag{20}$$

the coefficient b $(0 \leqslant b \leqslant 1)$ giving the strength, relative to the external stress amplitude $\Delta\sigma_0$, of the threshold stress amplitude below which no damage accumulation occurs. Notice that for $b = 0$ we recover the case investigated in Sec. III, whereas $b = 1$ leads to no damage accumulation infinitely far from the crack tips.

A similar analysis to the one performed in Sec. III shows that Eqs. (9) and (10) now read

$$\delta t(a_n) = \frac{F_{\text{thr}}(1-G_n)}{f_0[\Delta\sigma_{\text{eff}}(a_{n+1};a_n)]^\gamma} \tag{21}$$

and

$$G_n = \sum_{k=1}^{n} h_{nk}(1-G_{k-1}), \tag{22}$$

with the g_{nk} of Eq. (10) replaced by

$$h_{nk} \equiv \left[\frac{\Delta\sigma_{\text{eff}}(a_0+(n+1)\delta r; a_0+(k-1)\delta r)}{\Delta\sigma_{\text{eff}}[a_0+k\delta r; a_0+(k-1)\delta r]}\right]^\gamma, \tag{23}$$

whose asymptotic behavior is given by

$$h_{nk} \approx \begin{cases} \left[\frac{(1-b)\sqrt{2a_0\delta r}}{a_0-b\sqrt{2a_0\delta r}}\right]^\gamma, & k\delta r \ll a_0 \ll n\delta r; \\ \left[\frac{(1-b)\sqrt{2k}}{k-b\sqrt{2k}}\right]^\gamma, & a_0 \ll k\delta r \ll n\delta r; \\ (n-k+2)^{-\gamma/2}, & a_0 \ll k\delta r \approx n\delta r. \end{cases} \tag{24}$$

Thus, Eq. (15) remains valid for $\gamma > \gamma_c$, and we still have $m = \gamma$, with $\gamma_c = 2$ irrespective of the value of b.

On the other hand, in the limit of small damage-accumulation exponent ($\gamma \to 0^+$), the expansion in Eq. (16) becomes

$$G_n \approx 1 + \ln\left(\frac{h_{n1}}{h_{n-1\,1}}\right), \; n > 1. \tag{25}$$

Now we have to distinguish between the cases $0 \leqslant b < 1$ and $b = 1$. If $0 \leqslant b < 1$, then

$$\frac{h_{n,1}}{h_{n-1,1}} \approx 1 - \gamma\left(\frac{a_0}{\delta r}\right)^2 \frac{1}{(1-b)} n^{-3}, \tag{26}$$

so that

$$1 - G_n \sim \gamma a_n^{-3}, \tag{27}$$

whereas if $b = 1$ we have

$$\frac{h_{n,1}}{h_{n-1,1}} \approx 1 - 2\gamma a_n^{-1}, \tag{28}$$

and thus

$$1 - G_n \sim \gamma a_n^{-1}. \tag{29}$$

Therefore,

$$m(\gamma \to 0) = \begin{cases} 6, & 0 \leqslant b < 1, \\ 2, & b = 1. \end{cases} \tag{30}$$

Numerical calculations suggest that for $0 < \gamma < 2$, a Paris regime still exists, but with a nonlinear relation between m and γ if $0 < b < 1$; see Fig. 8.

V. INTRODUCING DISORDER IN THE FATIGUE THRESHOLDS

In this section, we turn our attention to a description of crack growth in a heterogeneous medium by introducing disorder in the fatigue thresholds. We assume that the element at position x along the crack line has a fatigue threshold $F_{\text{thr}}(x)$ chosen randomly from the uniform probability distribution

$$P(F_{\text{thr}}) = \frac{1}{\Delta F}\theta(F_2 - F_{\text{thr}})\theta(F_{\text{thr}} - F_1), \tag{31}$$

where $\theta(x)$ is the Heaviside step function and $\Delta F \equiv F_2 - F_1$ gauges the disorder strength, with the additional condition that, in appropriate units, $F_1 + F_2 = 2$. We also assume that the fatigue thresholds at different elements are uncorrelated.

In the presence of disorder, elements far from the crack tips may reach their fatigue thresholds, giving rise to secondary

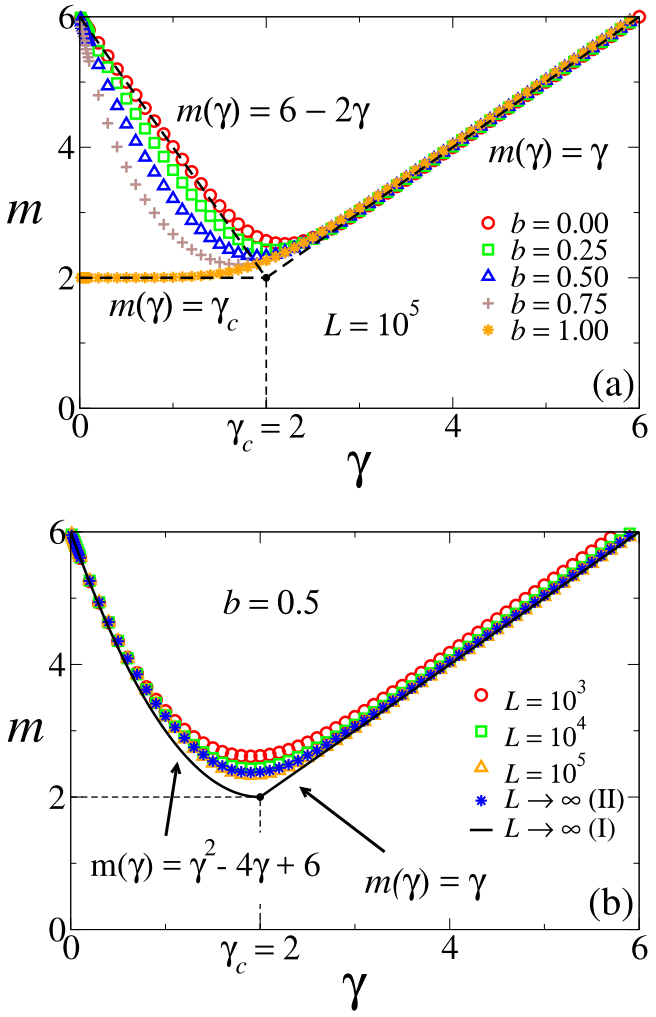

FIG. 8. Top: numerical dependence of the Paris exponent m on the damage-accumulation exponent γ, within the modified version of the model, for a few values of the threshold-stress-range parameter b and system size $L = 10^5$. Notice that the linear relation $m = \gamma$ seems to be recovered for $\gamma > 2$, but a nonlinear relation seems to emerge for $\gamma < 2$ if $0 < b < 1$. Bottom: finite-size behavior of m against γ for $b = 0.5$. The continuous curve is a polynomial guess for the infinite-size behavior. Blue stars indicate the results obtained by the alternative finite-size-scaling scheme employing Eq. (8).

cracks, as illustrated in Fig. 9. In such a case, we focus on the growth of the initial or main crack, noting that it may coalesce with secondary cracks as the growth dynamics proceeds.

After the rupture of n elements, we label the configuration of the system as

$$\{a_k,\overline{x}_k\}_n, \tag{32}$$

where a_k is the half-length of the kth crack, which is centered at position $\overline{x}_k$ with respect to the midpoint of the initial crack. We assume that between rupture events, an element at position x is subject to damage accumulation following

$$\delta F(x;\{a_k,\overline{x}_k\}_n) = f_0\delta t(\{a_k,\overline{x}_k\}_n)[\Delta\sigma(x;\{a_k,\overline{x}_k\}_n)]^\gamma, \tag{33}$$

where $\delta t(\{a_k,\overline{x}_k\}_n)$ is the time elapsed between the nth and the $(n+1)$th rupture events, and $\Delta\sigma(x;\{a_k,\overline{x}_k\}_n)$ is the

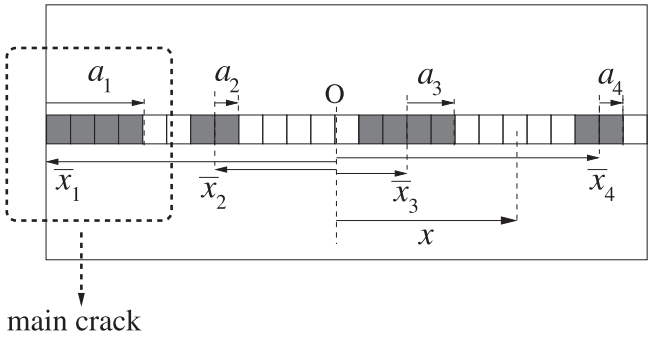

FIG. 9. Schematic diagram representing a configuration of the system with random fatigue thresholds. In this case, we observe the presence of multiple cracks (each one indicated by a sequence of dark elements) along the propagation line.

corresponding stress amplitude at position x. This is analogous to Eq. (4), so that, in the notation of Sec. IV, we take $b = 0$.

As a rupture event involves the element requiring the least time to reach its fatigue threshold, the analog of Eq. (5) allows us to write $\delta t(\{a_k,\overline{x}_k\}_n)$ as

$$\delta t(\{a_k,\overline{x}_k\}_n) = \min_x\left\{\frac{F_{\rm thr}(x) - F(x;\{a_k,\overline{x}_k\}_{n-1})}{f_0[\Delta\sigma(x;\{a_k,\overline{x}_k\}_n)]^\gamma}\right\}. \tag{34}$$

It should be emphasized that, as soon as the first secondary crack appears, the stress amplitude $\Delta\sigma(x;\{a_k,\overline{x}_k\}_n)$ is no longer given by the analog of the simple form in Eq. (2). Due to the lack of an analytical solution for the stress field of multiple thin cracks, even in the simplest case in which the cracks are arranged along the same line, we resort to an independent-crack approximation, to be detailed below, whenever it is necessary to deal with secondary cracks, except in the case $\gamma = 0$, which we now present in detail.

A. The case $\gamma = 0$

In this limit, damage accumulation is independent of the local stress amplitude, so that the problem is similar to a 1D percolation process, and it is possible to obtain analytical results. In this subsection only, in order to simplify the calculations, we assume that the initial crack is a notch of length a_0 at the left end of the medium. The case of a central initial crack was briefly discussed in Ref. [10].

The probability of finding the main crack with length a at time t is given by

$$P(a|a_0,t) = [p(t)]^{a-a_0}[1 - p(t)], \tag{35}$$

in which $p(t)$ is the probability that an element has reached its fatigue threshold before time t, the factor $1 - p(t)$ being the probability that the element at the (right) tip of the main crack remains intact at time t. Since for $\gamma = 0$ we have $F(x;\{a_k,\overline{x}_k\}_n) = f_0 t$, it follows that

$$p(t) = \min\left\{1, \frac{t - t_1}{T}\theta(t - t_1)\right\}, \tag{36}$$

where $t_1 = F_1/f_0$ and $T = \Delta F/f_0$ are parameters related to the disorder distribution.

For a semi-infinite medium, the average length of the main crack at time t is given by

$$\langle a\rangle_t = \sum_{a=a_0}^{\infty} a\,P(a|a_0,t) = a_0 + \frac{p(t)}{1-p(t)}, \tag{37}$$

so that, eliminating t from Eqs. (36) and (37), the average tip velocity of the main crack can be written, for $t_1 < t < t_2 \equiv F_2/f_0$, as

$$\langle v\rangle_t = \frac{d}{dt}\langle a\rangle_t \sim \langle a\rangle_t^2, \tag{38}$$

implying a Paris exponent $m = 4$ instead of $m = 6$ as in the uniform limit.

It is also possible to study finite systems containing L elements, and have access to the distribution of waiting times between rupture events, as well as to the distribution of avalanche sizes. An avalanche is defined as a sudden event in which the crack tip advances by more than a single discretized elements, while the avalanche size is the number of elements by which the main crack grows in a single event. (Notice that an avalanche involves stress rearrangements by changing the configuration of the cracks in the system. In the limit of $\gamma = 0$, this stress rearrangement is irrelevant for damage accumulation, and avalanches are just random nucleations. This is not the case for any $\gamma > 0$, and avalanche events will be correlated.). Toward that end, we must consider the probability that the main crack has length a and, upon rupture of the element at its tip, happening between times t and $t + dt$, advances Δa elements having waited a time between Δt and $\Delta t + d(\Delta t)$ since it last advanced. Denoting this probability by $\rho_{_L}(\Delta a,\Delta t,t|a)\,dt\,d(\Delta t)$, we have

$$\begin{aligned}\rho_L(\Delta a,\Delta t,t|a) = {}& \frac{(a-a_0)(a-a_0+1)}{T^2}[p(t-\Delta t)]^{a-a_0-1} \\ & \times [p(t)]^{\Delta a-1}\{[1-p(t)](1-\delta_{\Delta a,L-a}) \\ & + \delta_{\Delta a,L-a}\},\end{aligned} \tag{39}$$

$\delta_{i,j}$ being the Kronecker delta symbol. Here, $[p(t-\Delta t)]^{a-a_0-1}$ is the probability that $a-a_0-1$ elements are broken at time $t-\Delta t$, $d(\Delta t)/T$ is the probability that the previous growth event of the main crack has occurred between times $t-\Delta t$ and $t-\Delta t+d(\Delta t)$, dt/T is the probability that the new growth event of the main crack occurs between times t and $t+dt$, and $[p(t)]^{\Delta a-1}$ is the probability that the first $\Delta a-1$ elements to the right of the element at the crack tip are broken before time t. The terms between curly brackets in Eq. (39) distinguish the case in which the crack stops before reaching the right end of the medium, which occurs with probability $1-p(t)$, from the case in which catastrophic failure occurs, corresponding to $\Delta a = L-a$. The prefactor on the right-hand side of Eq. (39) ensures normalization.

The marginal probabilities for avalanche sizes and waiting times are obtained from $\rho_L(\Delta a,\Delta t,t|a)$ by integrating over the appropriate variables. The marginal probability for avalanche sizes Δa is given by

$$\begin{aligned}P_L(\Delta a|a) &= \int_{t_1}^{t_2} dt \int_0^{t-t_1} d(\Delta t)\rho_L(\Delta a,\Delta t,t|a) \\ &= (a-a_0+1)\left[\frac{1-\delta_{\Delta a,L-a}}{(\Delta a+a-a_0+1)(\Delta a+a-a_0)}\right. \\ &\quad \left. + \frac{\delta_{\Delta a,L-a}}{L-a_0}\right],\end{aligned} \tag{40}$$

while the marginal probability for waiting times between consecutive jumps is

$$\begin{aligned}P_L(\Delta t|a) &= \sum_{\Delta a=1}^{L-a}\int_{t_1}^{t_1+\Delta t} dt\rho_L(\Delta a,\Delta t,t|a) \\ &= \frac{(a-a_0+1)}{T}\left(1-\frac{\Delta t}{T}\right)^{a-a_0}.\end{aligned} \tag{41}$$

The mean values of avalanche sizes, $\langle\Delta a\rangle_{a,L}$, and waiting times, $\langle\Delta t\rangle_{a,L}$, can be computed from the above marginal probabilities, yielding

$$\begin{aligned}\langle\Delta a\rangle_{a,L} = {}& (a-a_0+1)\big[\big(H_{L-a_0}-H_{a-a_0}\big)\big(1-\delta_{a,a_0}\big) \\ & + H_{L-a_0}\delta_{a,a_0}\big],\end{aligned} \tag{42}$$

where H_n is the harmonic number of order n, and

$$\langle\Delta t\rangle_{a,L} = \frac{T}{a-a_0+2}. \tag{43}$$

Figure 10 compares these last results with numerical simulations implementing the crack-growth dynamics in the limit $\gamma = 0$.

The ratio between those mean values yields an estimate of the crack-growth rate, proportional to the the crack-tip velocity of the main crack, which we define as

$$\begin{aligned}\langle v\rangle_{a,L} = \frac{\langle\Delta a\rangle_{a,L}}{\langle\Delta t\rangle_{a,L}} &= \frac{(a-a_0+2)(a-a_0+1)}{T} \\ &\times\big[\big(1-\delta_{a,a_0}\big)\big(H_{L-a_0}-H_{a-a_0}\big)+\delta_{a,a_0}H_{L-a_0}\big].\end{aligned} \tag{44}$$

Thus, in the limit of large crack lengths ($L \gg a \gg a_0$), we obtain

$$\langle v\rangle_{a,L} \sim a^2 \ln\left(\frac{L}{a}\right), \tag{45}$$

leading to a Paris law with exponent $m = 4$, apart from logarithmic corrections depending on the system size. Numerical simulations of the model are in good agreement with the analytical calculations, as shown in Fig. 11.

B. The case $\gamma > 0$

In this subsection, we study the properties of the disordered model in situations in which the damage-accumulation exponent is nonzero, a case in which a fully analytical treatment is impossible. The approach we employ is therefore mostly numerical, and based on an *independent-crack approximation* that neglects the correlations between the multiple cracks emerging along the propagation line during the breaking process.

Our approximate results can be compared with another approach, the *fuse model* [18,19], which is equivalent to

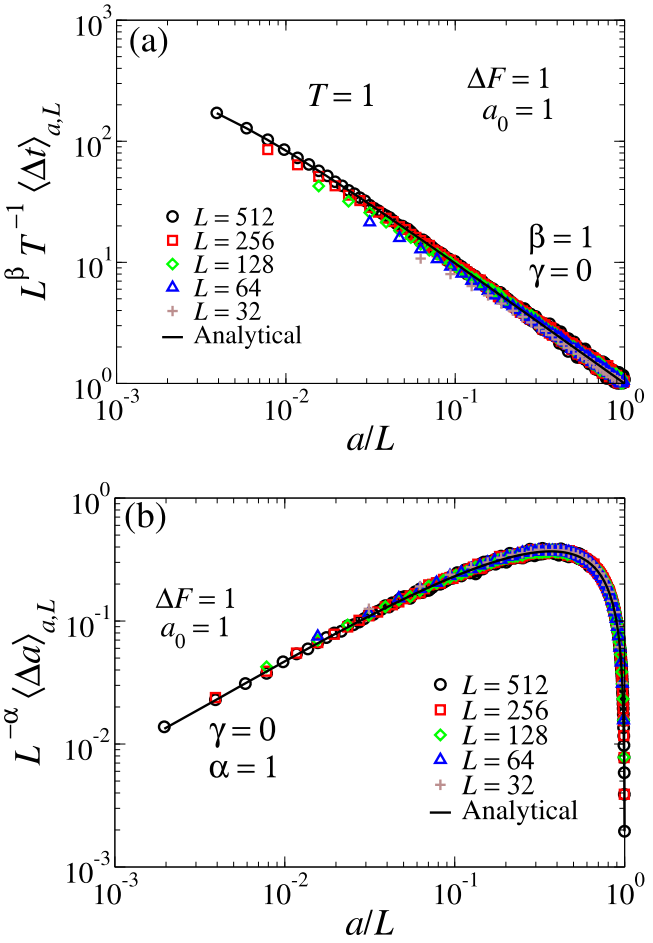

FIG. 10. Rescaled mean values of waiting times (top) and avalanche sizes (bottom) between consecutive jumps of the main crack for the disordered version of the model with $\gamma = 0$. Numerical results are in good agreement with the analytical results from Eqs. (42) and (43), indicating power-law behaviors of both quantities as functions of the length of the main crack, in the limit of infinite system size.

fracturing a discretized scalar version of linear-elastic theory, appropriate for the loading mode and the two-dimensional geometry we assume here. Within the fuse model, we can compute numerically the finite-size value of the local stress in multicrack configurations.

The independent-crack approximation (ICA) consists in writing the stress (and thus also the stress amplitude) in the element located at position x when the multicrack configuration is $\{a_k,\overline{x}_k\}_n$ as

$$\sigma(x;\{a_k,\overline{x}_k\}_n) \simeq \sigma_0 + \sum_{k=1}^{N}[\sigma_1(x;\overline{x}_k,a_k) - \sigma_0],$$

$$x \notin \bigcup_{k=1}^{N}(\overline{x}_k - a_k,\overline{x}_k + a_k), \tag{46}$$

in which σ_0 is the applied external stress, a_k is the half-length of the kth crack, which is centered at position $\overline{x}_k$ with respect to the midpoint of the initial crack (which we assume again to be located at the center of the system), and $\sigma_1(x;\overline{x}_k,a_k)$ is the

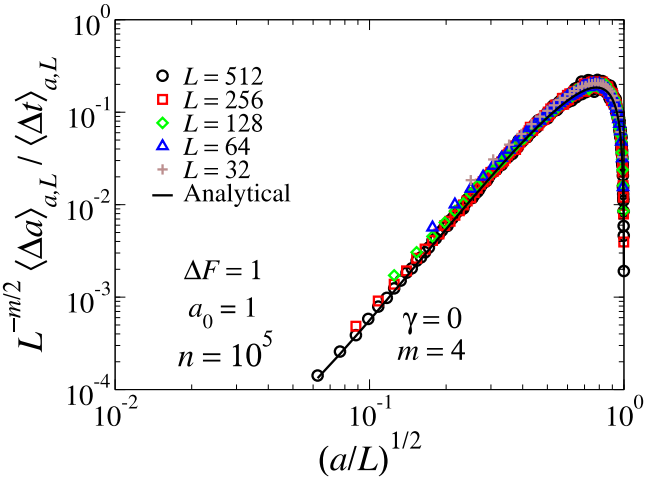

FIG. 11. Rescaled mean crack-growth rate defined as the ratio between the mean values of avalanche size and the waiting time between consecutive jumps for the disordered version of the model with $\gamma = 0$. Numerical results are in good agreement with the analytical prediction of Eq. (44), indicating a Paris exponent equal to $m = 4$ in the limit of infinite system size.

stress field that would be produced by the kth crack if it were the only crack in the system. The $-\sigma_0$ factors inside the square brackets on the right-hand side of Eq. (46) ensure that very far from any cracks, the external stress is recovered. Inside any of the cracks, the stress is zero.

To get an idea about the accuracy of the ICA, we compare its predictions with those of the fuse model for the case in which there are two symmetric cracks with length $2a$ whose centers are separated by d elements. The numerical comparison is shown in Fig. 12, and it indicates good qualitative and quantitative agreement, with a relative error of at most a few percent.

We now discuss the results obtained by implementing the disordered crack-growth model according to the ICA with $\gamma > 0$, presenting comparisons with the random-fuse model whenever appropriate. In our simulations, we performed averages over up to 100 000 disorder realizations, with system sizes ranging from $L = 2^5$ to 2^9. We varied the damage-accumulation exponent γ and the disorder strength ΔF. The single-crack stress fields $\sigma_1(x;\overline{x}_k,a_k)$ were calculated from Eq. (2).

First we note that it can be shown (see Ref. [8]) that for $\gamma < 2$ any amount of disorder leads to the appearance of secondary cracks, while for $\gamma > 2$ those appear only for stronger disorder, such that $F_1/F_2 \lesssim 1 - 1/\zeta(\frac{1}{2}\gamma)$, which, in terms of the disorder strength ΔF, corresponds to

$$\Delta F > \Delta F_{\min} \simeq \frac{2}{2\zeta\left(\frac{1}{2}\gamma\right) - 1}. \tag{47}$$

The value of $\Delta F_{\min}$ increases monotonically from 0 at $\gamma = 2$ to 2 as $\gamma \to \infty$, which implies that, for large values of γ, secondary cracks appear only if the disorder distribution allows the presence of arbitrarily small local damage thresholds.

For all values of γ, both the average crack jump (avalanche size) Δa and the average waiting times between consecutive

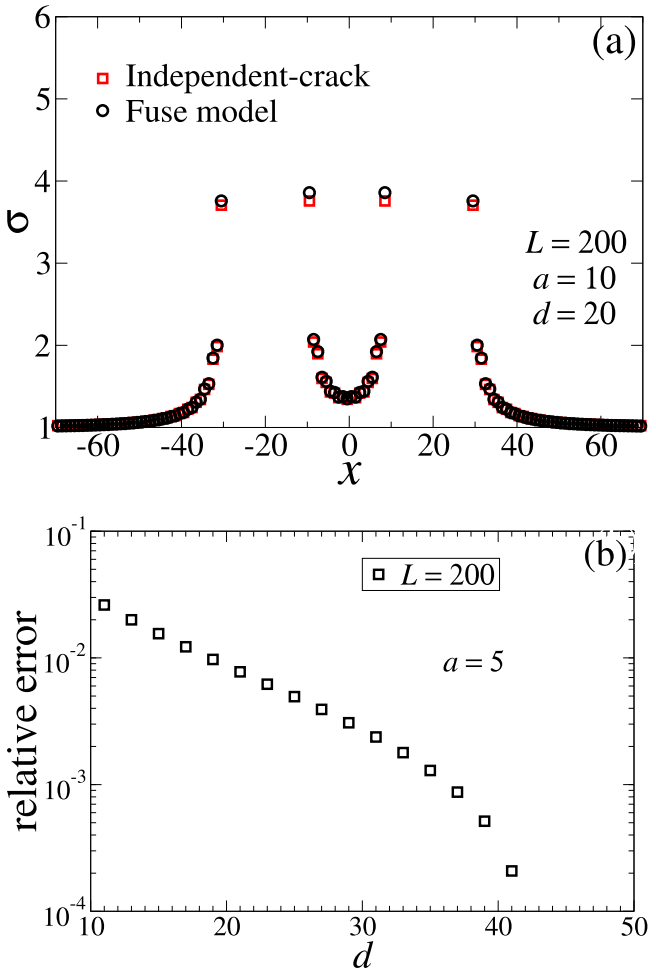

FIG. 12. Top: comparison between the stress along the propagation line of the system calculated exactly (black circles) and by the independent-crack approximation (red squares) for a sample of length L containing two cracks of length $2a$ separated by a distance d. Both calculations were performed for the fuse model, which is equivalent to fracturing a discretized scalar linear-elastic theory (see the main text). The independent-crack approximation uses the stress field calculated within the fuse model as if each crack would be separately present in the system. Bottom: relative error between the exact result and the independent-crack approximation for the stress at the crack tip, as a function of the separation d between cracks of length $2a$.

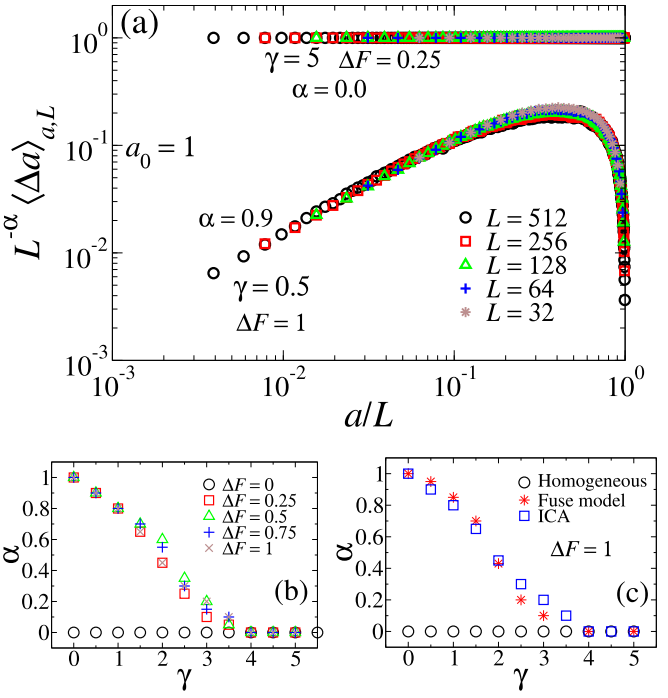

FIG. 13. Top: scaling plot of the average main crack jump $\langle \Delta a \rangle_{a,L}$ as a function of the rescaled crack half-length a/L, for different sample sizes ranging from $L = 2^5$ to 2^9 and two values of the damage-accumulation exponent γ and the disorder strength ΔF. Bottom: dependence of the power-law exponent α on the damage accumulation exponent γ for different degrees of disorder, as predicted by the ICA (left) and comparison between predictions of the ICA and the random-fuse model for $\Delta F = 1$ (right).

jumps Δt seem to follow power laws of the main crack length $2a$, namely $\langle \Delta a \rangle_{a,L} \sim a^{\alpha}$ and $\langle \Delta t \rangle_{a,L} \sim a^{-\beta}$, as shown by the finite-size scaling plots of Figs. 13 and 14. The results for the corresponding exponents α and β are in good agreement with those predicted by the random-fuse model. Notice that α quickly becomes negligible for $\gamma > \gamma_c$, indicating that in this regime the formation of secondary cracks is rare, except in the presence of strong disorder ($\Delta F > \Delta F_{\min}$). As for the β exponent, it seems to be approximately given by $\gamma/2$ for $\gamma > 2$, while approaching $\beta = 1$ as $\gamma \to 0$.

Predictions of the ICA for the average crack growth rate of the main crack are shown in the finite-size scaling plots of Fig. 15, exhibiting the power-law behavior associated with the Paris law. The values of the Paris exponent are chosen so as to yield the best data collapse of the curves corresponding to different system sizes for the same values of the damage-accumulation exponent γ, with the help of Eq. (8). The dependence of the macroscopic Paris exponent m on the damage-accumulation exponent γ, for different degrees of disorder, is shown in Fig. 16, together with the results found for the homogeneous case [8] and the random-fuse model [10].

Notice that, in all the cases studied, we observed a strong tendency of the Paris exponent for $\gamma \lesssim 2$ to display a value $m(\gamma) \simeq 4$, irrespective of the disorder strength. This can be understood on the basis of the observation that, already in the uniform limit, $\gamma_c = 2$ separates a growth regime in which damage accumulation happens mostly around the crack tips ($\gamma > 2$) from another regime where damage accumulation accumulates more uniformly along the propagation line ($\gamma < 2$). It is thus not surprising that, upon the introduction of random damage thresholds, this last regime is dominated by disorder effects, rather than by the relatively small variations in damage accumulation along the propagation line, therefore leading to $m = 4$, as in the $\gamma \to 0$ limit. On the other hand, for $\gamma \gtrsim 4$ the Paris exponent $m(\gamma)$ assumes values very close to the uniform-limit result γ, as already observed in the random-fuse calculations [10]. The region $2 \lesssim \gamma \lesssim 4$ is plagued by large statistical fluctuations and corrections to scaling, making it difficult to locate within this picture.

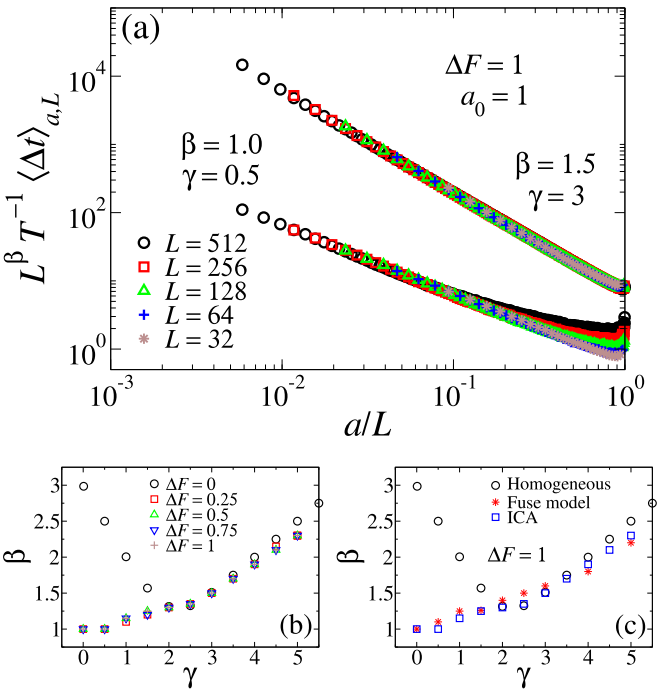

FIG. 14. Top: scaling plot of the average waiting time between successive jumps of the main crack, $\langle \Delta t \rangle_{a,L}$, normalized by the average rupture time T, as a function of the rescaled half-length a/L, for different sample sizes ranging from $L = 2^5$ to 2^9 and a few values of the damage-accumulation exponent γ and $\Delta F = 1$. Bottom row: Dependence of the power-law exponent β on the damage accumulation exponent γ for different degrees of disorder, as predicted by the ICA (left) and comparison between predictions of the ICA and the random-fuse model for $\Delta F = 1$ (right).

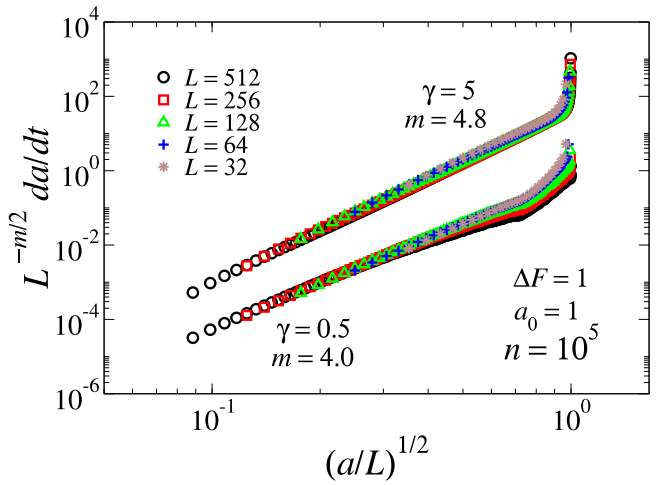

FIG. 15. Scaling plot of the main crack-growth rate da/dt as a function of the crack rescaled half-length a/L, for different system sizes (from $L = 2^5$ to 2^9) and a few values of the damage-accumulation exponent γ. The disorder strength is fixed at $\Delta F = 1$. Curves for $\gamma = 5$ are offset for clarity. To minimize statistical fluctuations, crack-growth rates were calculated from the numerical derivative of the half-crack length with respect to the average time in which the crack became trapped in a configuration with the corresponding length. Averages were taken over $n = 10^5$ disorder realizations.

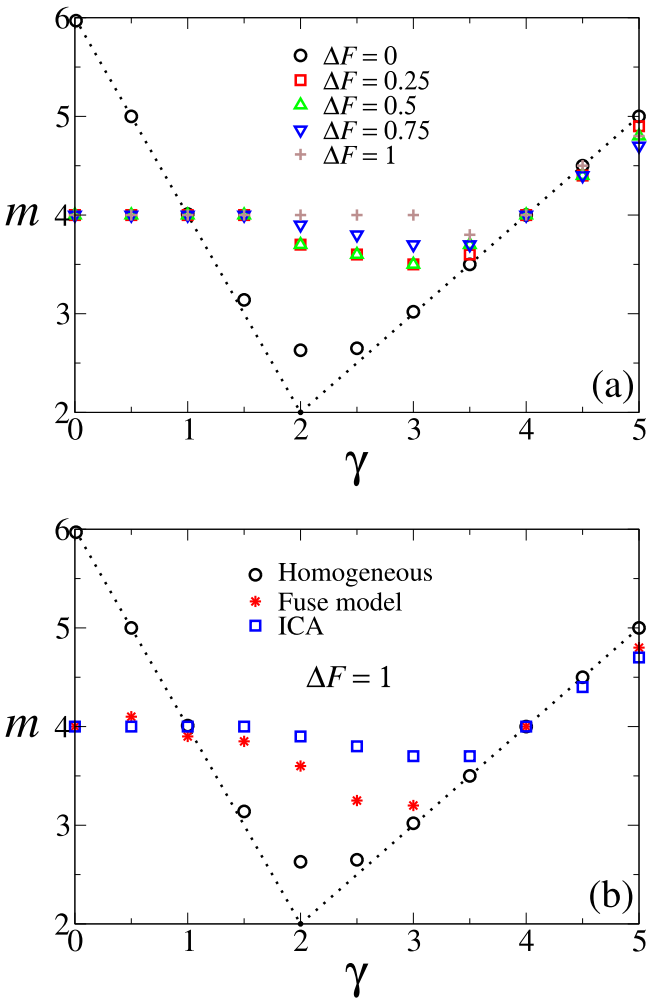

FIG. 16. Top: dependence of the Paris exponent m on the damage-accumulation exponent γ for the disordered model, according to the independent-crack approximation. Bottom: comparison between the results obtained by the independent-crack approximation and the random-fuse model for the same relation $m \times \gamma$, with disorder strength $\Delta F = 1$. Notice the good agreement except in the vicinity of $\gamma = 2$.

VI. HEALING EFFECTS IN THE UNIFORM LIMIT

We finally return briefly to the uniform limit, and we introduce the possibility of damage healing with a characteristic time τ. Explicitly, we assume that, up to time t, the accumulated damage on the element located at position x is given by [20]

$$F(x;t) = f_0 \int_0^t dt' [\Delta\sigma(x;t')]^{\gamma} e^{-(t-t')/\tau}, \qquad (48)$$

where f_0 is a constant setting the time scale, $\Delta\sigma(x;t)$ is the stress amplitude at position x and time t, and γ is the damage amplification exponent. Healing mechanisms during fatigue crack growth are known to be relevant, for instance, in materials such as asphalt [21] and also in self-healing composite materials such as epoxy, with the incorporation of microencapsulated healing agents such as dicyclopentadiene [22]. The healing time τ is treated here as another

phenomenological parameter, which presumably depends on the temperature and possibly on the concentration of a healing agent.

Taking into account that $\Delta\sigma(x;t)$ does not vary between crack-growth events, the last equation leads to a recursion relation for the damage at a given location when the crack has length $2a$,

$$F(x;a) = e^{-\delta t(a)/\tau} F(x;a-\delta r) + \delta F(x;a), \qquad (49)$$

with

$$\delta F(x;a) = f_0 \tau [\Delta\sigma(x;a)]^{\gamma} (1 - e^{-\delta t(a)/\tau}), \qquad (50)$$

where the symbols have the same meaning as in Sec. II, and we have used the fact that in the uniform limit, the crack always grows by the breaking of the elements at the crack tips. Notice that as $\tau \to \infty$, we recover Eqs. (4) and (5).

The time interval $\delta t(a)$ during which the crack has length $2a$ is determined from the condition $F(a+\delta r;a) = F_{\rm thr}$. For the time during which the crack remains with the initial notch size $2a_0$, this yields

$$\delta t(a_0) = -\tau \ln\left(1 - \frac{F_{\rm thr}}{f_0 \tau [\Delta\sigma(a_0+\delta r;a_0)]^{\gamma}}\right), \qquad (51)$$

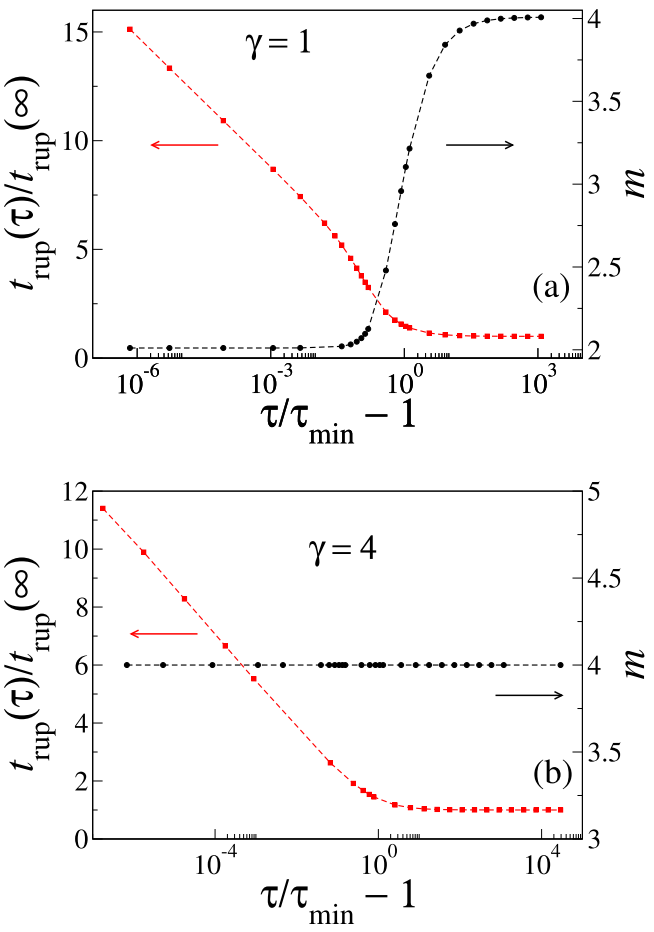

FIG. 17. Behavior of the rescaled rupture time (red curves) and the Paris exponents (black curves) as functions of the healing characteristic time τ, rescaled by the corresponding minimum value, for $\gamma = 1$ (top) and $\gamma = 4$ (bottom).

indicating the existence of a minimum value of τ below which the crack cannot grow. This minimum value is given by

$$\tau_{\rm min} = \frac{F_{\rm thr}}{f_0 [\Delta\sigma(a_0+\delta r;a_0)]^{\gamma}}. \qquad (52)$$

For a fixed value of τ, this result is compatible with the existence of a minimum stress amplitude around which the fatigue lifetime diverges [22].

Using the previous equations, we can numerically investigate the crack-growth dynamics and its dependence on the parameters γ and τ. It turns out that the Paris exponent m is independent of τ for $\gamma \geqslant 2$, but it becomes τ-dependent for $\gamma < 2$. In this last regime, m is equal to $6-2\gamma$ for $\tau \to \infty$, but it approaches the value 2 as τ approaches $\tau_{\rm min}$. Figure 17 shows, for $\gamma = 1$ and 4, the behavior of m as a function of τ for a finite sample with $L = 2^{15}$ elements. Also shown is the τ dependence of the rupture time $t_{\rm rup}$, normalized by its value in the limit $\tau \to \infty$. Notice the seemingly logarithmic divergence of $t_{\rm rup}$ as $\tau \to \tau_{\rm min}$, a prediction whose experimental verification would require an estimate of the healing time τ in terms of material and environmental parameters. At the moment, to the best of our knowledge, such estimates are not available.

VII. CONCLUSIONS

In summary, we investigated various extensions of a model for subcritical fatigue crack growth in which damage accumulation is assumed to follow a power law of the local stress amplitude. In all cases, our main interest was in determining the effects of model ingredients on the Paris exponent governing subcritical crack-growth dynamics at the macroscopic scale, starting from a single small notch propagating along a fixed line.

In the uniform limit, we showed that a number of analytical and numerical results can be established regarding the dependence of the Paris exponent on the damage-accumulation exponent, the threshold stress range required to induce local damage, and the characteristic time of damage healing. There is a critical value of the damage accumulation exponent, namely $\gamma_c = 2$, separating two distinct regimes of behavior for the Paris exponent m. For $\gamma > \gamma_c$, the Paris exponent is shown to assume the value $m = \gamma$, a result that proves robust against the introduction of various modifying ingredients. On the other hand, in the regime $\gamma < \gamma_c$ the Paris exponent is seen to be sensitive to the different ingredients added to the model, with rapid healing or a threshold stress amplitude $b = 1$ leading to $m = 2$ for all $\gamma < \gamma_c$, in contrast to the linear dependence $m = 6 - 2\gamma$ observed for very long characteristic healing times and $b = 0$.

The introduction of disorder on the local fatigue thresholds leads to the possible appearance of multiple cracks along the propagation line, and the Paris exponent tends to $m \simeq 4$ for $\gamma \lesssim 2$, while retaining the behavior $m = \gamma$ for $\gamma > 4$. The independent-crack approximation employed for all calculations in the presence of disorder yields results in good agreement with the more computationally expensive random-fuse calculations, suggesting that it can be reliably applied to further extensions of the model. An interesting candidate would be an investigation of the combined effects of disorder

and healing, a situation that is closer to what occurs in real materials.

It is possible to compare the results obtained from the present approach with those derived in recent years (see, e.g., Refs. [23–27]) based on the extension of ideas of incomplete self-similarity as applied directly to the macroscopic Paris law (see, e.g., Refs. [28,29] and references therein). These works point not only to the effect, on the Paris exponent, of characteristic lengths (usually the sample thickness) or of plasticity properties of the fracture-process zone ahead of the crack tip [28], but also to the fact that the fractal character of the crack profile leads to modifications of the asymptotic behavior of the stress field around the crack tip, which also affects the Paris law. Specifically, this changes the dependence of the stress field on the distance r to a thin crack tip, which now diverges as $r^{(D-2)/2}$, D being the fractal dimension of the crack profile [30]. Notice that this makes the stress field decay more slowly with r than the $r^{-1/2}$ behavior of a linear ($D = 1$) crack. This is reminiscent of the behavior of a damage-accumulation rule with $\gamma < 2$, for which, as discussed in Sec. III, damage is more uniformly distributed along the crack line. Therefore, a possible interpretation of the present approach is that, via the introduction of the damage-accumulation exponent γ, it encapsulates various effects such as the plasticity properties ahead of the crack tip and the fractal nature of the crack profile, allowing the use of linear-elastic fracture mechanics to provide an effective description of fatigue crack dynamics.

Incidentally, the question remains as to whether it is possible to relate the phenomenological, mesoscopic damage-accumulation exponent γ to atomistic or structural features of real materials. We are currently investigating the possibility of employing molecular dynamics or phase-field methods to approach this issue.

ACKNOWLEDGMENTS

We thank the Brazilian agencies FAPESP, CNPq, and National Institute of Science and Technology for Complex Systems in Brazil for their financial support. M.S.A. thanks Carmen Prado and André Timpanaro for useful discussions. We acknowledge financial support from the European Research Council (ERC) Advanced Grant No. 319968-FlowCCS and from NAP-FCx.

[1] S. Suresh, *Fatigue of Materials* (Cambridge University Press, Cambridge, 1998).
[2] D. L. Turcotte, *Fractal and Chaos in Geology and Geophysics*, 2nd ed. (Cambridge University Press, Cambridge, 1997).
[3] V. Bolotin, *Mechanics of Fatigue* (CRC, Boca Raton, FL, 1999).
[4] M. Marder, *Condensed Matter Physics*, 2nd ed. (Wiley, Hoboken, NJ, 2010).
[5] A. A. Griffith, Philos. Trans. R. Soc. London, Ser. A **221**, 163 (1921).
[6] U. Krupp, *Fatigue Crack Propagation in Metals and Alloys* (Wiley-VCH, Weinheim, 1998).
[7] P. Paris and F. Erdogan, J. Basic Eng. **85**, 528 (1963).
[8] A. P. Vieira, J. S. Andrade, Jr., and H. J. Herrmann, Phys. Rev. Lett. **100**, 195503 (2008).
[9] L. R. Botvina and G. I. Barenblatt, Strength Mater. **17**, 1653 (1985).
[10] C. L. N. Oliveira, A. P. Vieira, H. J. Herrmann, and J. S. Andrade, Jr., Europhys. Lett. **100**, 36006 (2012).
[11] M. J. Alava, P. K. V. V. Nukala, and S. Zapperi, Adv. Phys. **55**, 349 (2006).
[12] D. Krajcinovic, *Damage Mechanics* (Elsevier, Amsterdam, 1996).
[13] H. J. Herrmann and L. de Arcangelis, in *Disorder and Fracture*, edited by J. C. Charmet, S. Roux, and E. Guyon (Springer, Boston, 1990), pp. 149–163.
[14] H. J. Herrmann, Physica D **38**, 192 (1989).
[15] H. J. Herrmann, J. Kertész, and L. de Arcangelis, Europhys. Lett. **10**, 147 (1989).
[16] V. K. Horváth and H. J. Herrmann, Chaos, Solitons Fractals **1**, 395 (1991).
[17] W. Elber, ASTM STP **486**, 230 (1971).
[18] A. Gilabert, C. Vanneste, D. Sornette, and E. Guyon, J. Phys. **48**, 763 (1987).
[19] L. de Arcangelis, S. Redner, and H. J. Herrmann, J. Phys. Lett. **46**, 585 (1985).
[20] F. Kun, M. H. Costa, R. N. Costa Filho, J. S. Andrade, Jr., J. B. Soares, S. Zapperi, and H. J. Herrmann, J. Stat. Mech. (2007) P02003.
[21] Z. Si, D. N. Little, and R. L. Lytton, J. Mater. Civ. Eng. **14**, 461 (2002).
[22] E. N. Brown, S. R. White, and N. R. Sottos, Composites Sci. Technol. **65**, 2474 (2005).
[23] M. Ciavarella, M. Paggi, and A. Carpinteri, J. Mech. Phys. Solids **56**, 3416 (2008).
[24] M. Paggi and A. Carpinteri, Chaos, Solitons Fractals **40**, 1136 (2009).
[25] A. Carpinteri and M. Paggi, J. ASTM Int. **8**, 104105 (2011).
[26] M. Paggi and O. Plekhov, J. Mech. Eng. Sci. **228**, 2059 (2014).
[27] R. Jones, F. Chen, S. Pitt, M. Paggi, and A. Carpinteri, Int. J. Fatigue **82**, 540 (2016).
[28] R. O. Ritchie, Int. J. Fracture **132**, 197 (2005).
[29] G. I. Barenblatt, Int. J. Fracture **138**, 19 (2006).
[30] A. Yavari, S. Sarkani, and E. T. Moyer, Int. J. Fracture **114**, 1 (2002).